Large-Signal Look-Up Table Model for InP HEMTs Including Non-Quasi-Static and Impact Ionisation Effects

D. Schreurs, A. Orzati*, L. Pergola*, H. Benedickter*, O. Homan*, and W. Bächtold*

K.U.Leuven, Div. ESAT-TELEMIC, Kasteelpark Arenberg 10, B-3001 Leuven, Belgium
*Swiss Federal Institute of Technology, Laboratory of Field Theory and Microwave Electronics, Gloriastrasse 35, CH-8092 Zürich, Switzerland

Abstract—**We developed an efficient method to determine a large-signal look-up table model for InP HEMTs. By performing the measurements on a logarithmic frequency scale, we have a high resolution at lower frequencies to accurately characterise impact ionisation, and sufficient data points at millimetre wave frequencies to extract the non-quasi-static parameters.**

I. Introduction

InP HEMTs outperform the high-frequency performance of GaAs based MESFETs and HEMTs. Due to the higher substrate and processing cost compared to GaAs, their use is mainly oriented towards circuit applications at millimetre wave frequencies, where GaAs based devices can not meet the required specifications. For this reason, it is necessary to have a model that can accurately describe the non-linear behaviour of InP HEMTs at millimetre wave frequencies. However, the model should also be accurate at the lower frequencies to predict well all characteristics of frequency-shifting circuits such as frequency multipliers and mixers. An important physical phenomenon that is manifested in the DC and S-parameter characteristics in the lower GHz range is the so-called kink effect, which is caused by impact ionisation [1]. Impact ionisation occurs in InP HEMTs at lower drain-source voltages compared to GaAs based HEMTs, due to the lower bandgap of the InGaAs channel layer. This effect is hence noticeable at typical operating conditions of non-linear applications and should therefore be included in the non-linear model representation.

There are already reported approaches to model FET-type devices, but these are either limited to verifications at microwave frequencies [2], [3], to a bias-dependent small-signal model [4], [5], or to GaAs based FETs [6], where impact ionisation is normally not considered.

In this work, we present a way to determine a large-signal look-up table model for InP HEMTs that is valid from DC up to millimetre wave frequencies. As InP HEMTs are standardly low-power devices, they are primarily used in low-power non-linear applications, such as mixers and frequency multipliers, and less in power applications. For this type of circuits, it is important to predict well the higher order harmonics and intermodulation products, but issues such as heating can be considered as second order.

We first present the reasoning of the used small-signal and large-signal equivalent scheme topologies in Section II, before we outline in detail the modelling procedure in Section III. In Section IV, we show the results of both small-signal and large-signal experimental model validation.

II. (Non-)linear equivalent circuit model

The modelling procedure can be considered as an extension of the GaAs PHEMT modelling method that we published earlier [7]. In that paper, where only experimental results at microwave frequencies were shown, we proposed a non-quasi-static small-signal and corresponding large-signal equivalent scheme where the feedback elements were replaced by transelements. To model InP HEMTs up to millimetre wave frequencies, this small-signal equivalent scheme needs to be extended. The first modification is that we split the extrinsic gate and drain pad capacitances in two to incorporate the distributed effect of the access transmission lines [4], [5]. Secondly, we add a network at the drain side to model the impact ionisation effect [8]. It is a parallel branch consisting of a resistance R_{im} in series with the parallel connection of a transconductance g_{im}, controlled by the intrinsic drain-gate voltage V_{dgi}, and a capacitance C_{im}. The complete small-signal equivalent network is represented in Figure 1.

The intrinsic large-signal equivalent scheme that is consistent with the basic intrinsic small-signal equivalent scheme consists of a parallel connection of a charge source and a current source at the drain, a current source at the gate, and a charge source in series with a bias-dependent resistor at the gate. The split of the pad capacitances does not influence this schematic, because they are part of the extrinsic network. More important is to find a consistent large-signal representation of the additional impact ionisation network. Based on our experiments, we found out that this can be treated as a first order dispersive network. The principle is similar to the incorporation of the low-frequency dispersive behaviour of G_m and G_{ds} in the kHz-MHz frequency range [9]. This means that we extract two times the bias-dependent G_m and G_{ds} values. The first extractions are based on frequencies which are on one hand higher than the low-frequency dispersive frequency range and on the other hand smaller than the frequency range over which the impact ionisation effect affects the S-parameter characteristics, which typically corresponds to 45 MHz-0.5 GHz. The second series of extractions are performed at frequencies where the impact ionisation effect is no longer present, which typically corresponds to frequencies above 7 GHz. After the integration of G_m and G_{ds} towards their respective intrinsic terminal voltages, the first part leads to a drain current denoted by I_{dsLF} and the second part to I_{dsHF}. The intrinsic large-signal model is shown in Figure 2. In this representation, we do not integrate the capacitances towards charges, but directly use the bias-dependent capacitances. At the gate side, where charge conservation is physically valid, this is mathematically equivalent, al-

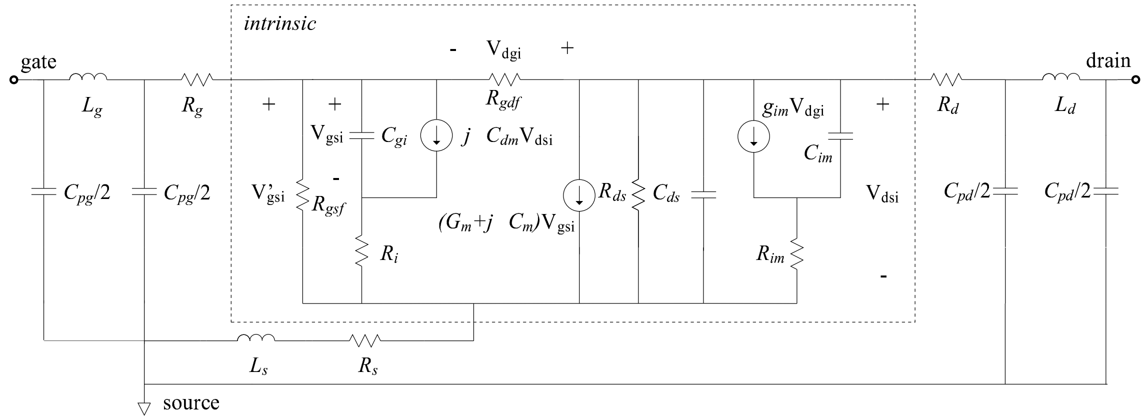

Fig. 1. Small-signal equivalent circuit for InP HEMTs incorporating non-quasi-static and impact ionisation effects.

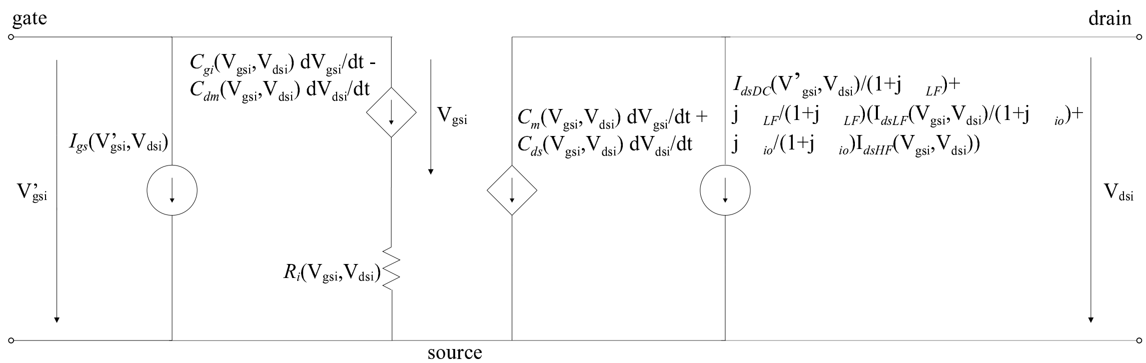

Fig. 2. Intrinsic large-signal model for InP HEMTs including non-quasi-static and impact ionisation effects.

though one has to be aware of possible peculiarities in practical situations [10]. At the drain side, charge-conservation is not necessarily guaranteed, because there we have a mixture of capacitances with different physical meanings. C_{ds} can be related to the combination of a space charge capacitance and a fringing capacitance within the device, whereas the transcapacitance C_m is a representation for the intrinsic time delay τ. This large-signal representation can be completed by adding a first-order transfer function to model the transition between the DC measured drain current I_{dsDC} and the I_{dsLF}, due to the low-frequency dispersion in the kHz and MHz frequency range [9]. Finally, note that the DC currents I_{gs} and I_{dsDC} are expressed as function of the total intrinsic gate voltage $V_{gsi}^{'}$ and not as function of the gate voltage V_{gsi} across C_{gs}.

After motivating the equivalent networks' topologies, we present in the next section the actual modelling procedure.

III. Modelling procedure

The modelling procedure consists of three major steps. First, the bias-(in)dependent small-signal elements are extracted from multi-bias S-parameter measurements. Next, the necessary integrations towards the corresponding state-functions are performed and finally, the model is implemented in a millimetre wave circuit simulator.

The first step is the determination of the extrinsic, bias-independent elements. These are extracted from cold S-parameter measurements using a procedure that we especially developed for HEMTs [11]. The major difference with similar methods for MESFETs is that this method does not require measurement data which are taken at conditions where a large positive gate current flows.

Subsequently, S-parameter measurements are performed at a grid of gate and drain voltages. A known drawback of look-up table models [2] is that the model accuracy of especially the higher harmonics can be largely influenced by the way the look-up tables are interpolated. For this reason, we use a non-equidistant grid with a global step of 50 mV for V_{gs} and of 100 mV for V_{ds}, but decrease this to 25 mV and 50 mV for V_{gs} and V_{ds}, respectively, when data are taken close to V_T and in the linear region. An alternative option is to represent the state-function by an empirical expression, of which the higher order derivatives are well defined. Since the drain current is the most important non-linear element, it would be sufficient to only replace the look-up table of the drain current by an empirical formula and to maintain the tables for the other non-linear elements.

In order to have a high accuracy from DC up to above 100 GHz, S-parameter measurements at a single frequency, as in [2], are not sufficient. On the other hand, a linear frequency sweep is not efficient, because a relatively high number of frequency points, e.g., 201, is needed in order to characterise well the frequency-dependent behaviour of impact ionisation. Therefore, we measure on a logarithmic frequency scale, such that we get sufficient information at low frequencies to extract the impact ionisation related parameters, and a small number of data points at millimetre wave frequencies, which is sufficient to extract the non-quasi-static related parameters. The intrinsic small-signal elements are calculated using the following equations:

$$G_{ds} = \mathrm{Re}\left(Y_{22}\right) \tag{1}$$
$$G_m = \mathrm{Re}\left(Y_{21} - Y_{12}\right) \tag{2}$$
$$R_i = \mathrm{Re}\left(1/\left(Y_{11} - Y_{11_0}\right)\right) \tag{3}$$
$$C_{gi} = -1/\left(2\pi \text{ freq } \mathrm{Im}\left(1/Y_{11}\right)\right) \tag{4}$$
$$C_{dm} = C_{gi} \text{ Mag}\left(\frac{Y_{12}}{Y_{11}}\right) \tag{5}$$
$$C_{ds} = -1/\left(2\pi \text{ freq } \mathrm{Im}\left(1/Y_{22}\right)\right) \tag{6}$$
$$C_m = \mathrm{Im}\left(Y_{21} - Y_{12}\right)/\left(2\pi \text{ freq}\right) \tag{7}$$
$$\tau_{io} = 1/\text{freq}|_{\mathrm{Min}(Y_{22})} \tag{8}$$

where Y_{11_0} denotes the DC value of Y_{11}. This is subtracted, because the I_{gs} state-function is directly measured at DC. This can be done because no I_{gs} frequency dispersion can be physically expected. A second reason is that the extraction of the small-signal resistances R_{gsf} and R_{gdf}, which correspond to the large-signal I_{gs}, is illy conditioned due to the very low gate current at most considered bias conditions. The extractions of the G_m and R_{ds} values that after integration lead to I_{dsLF} are performed at the lowest measurable frequency. The R_{ds} that corresponds to I_{dsHF} is determined at the frequency defined by $1/\tau_{io}$. The HF G_m and the other intrinsic elements can well be determined by taking the mean over the 10 GHz - 25 GHz frequency range, hence at microwave frequencies and well above the frequency range where dispersive effects might occur.

We implemented both the measurement and extraction parts in ICCAP. An advantage of this software package is the ease to define a logarithmic frequency scale. Also, we systematically perform DC measurements and a couple of standard S-parameter measurements before and after the series of multi-bias S-parameter measurements. In this way, we check whether the device has been gradually degrading [12]. If this would be the case, the gathered data do not longer lead to a model which is representative for the considered technology. The appropriate solution is hence to adapt the multi-bias grid accordingly. Finally, we implemented the model as a so-called "Symbolically Defined Device" in the ADS high-frequency circuit simulator.

IV. Experimental validation

The accuracy and limitations of the model have been evaluated at both the small- and large-signal level.

The first validation is to check the model under small-signal operation. Figure 3 presents the comparison of measured and simulated S-parameters at a DC bias condition where the impact ionisation effect is clearly present. This effect is reflected in the S-parameters by means of an inductive S_{22} and a decreased S_{21} at lower frequencies. The S_{21} is represented both on a polar plot and on a dB-scale to better visualise the impact ionisation effect. We notice that a first-order transfer function models the transition between the I_{dsLF} and I_{dsHF} sufficiently well.

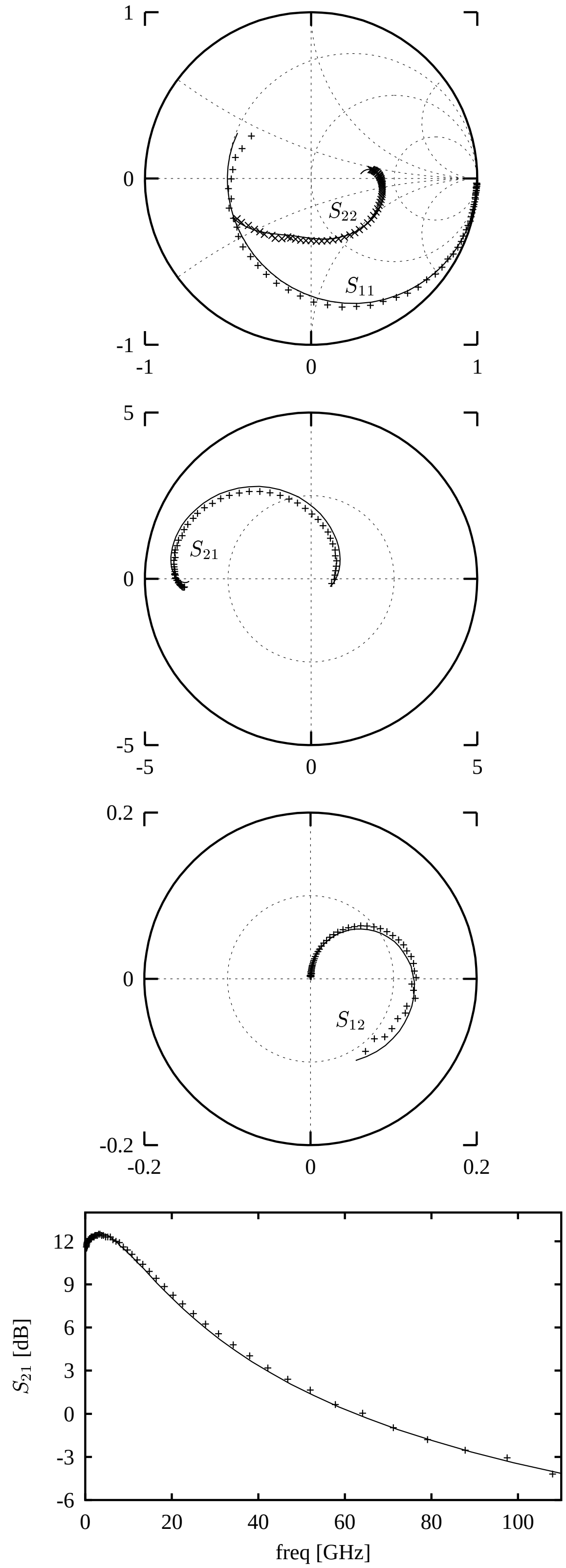

Fig. 3. Comparison between measured (symbols) and simulated (__) S-parameters at (V_{gs}, V_{ds}) = (-0.2 V, 1.4 V).

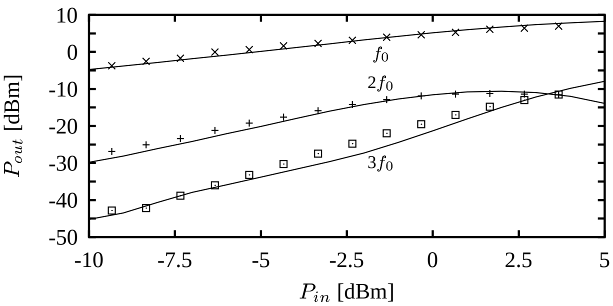

Fig. 4. Measured (symbols) and simulated (__) output power versus input power at the fundamental frequency of 16 GHz and the corresponding second and third harmonics. The DC bias condition is (V_{gs}, V_{ds}) = (-0.3 V, 1 V).

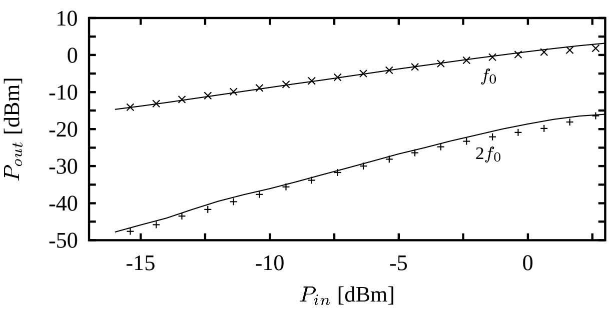

Fig. 5. Measured (symbols) and simulated (__) output power versus input power at the fundamental frequency of 32 GHz and the corresponding second harmonic. The DC bias condition is (V_{gs}, V_{ds}) = (-0.3 V, 0.7 V).

Consequently, we have verified the prediction of the output power at several fundamental frequencies and DC operating conditions. Figure 4 compares the measured and simulated output power of the first three harmonics at a fundamental frequency of 16 GHz. We notice that even the third harmonic is well modelled, which means that the grid of DC voltages at which S-parameters are taken is properly chosen. Figure 5 shows the good results of the fundamental and second harmonic output power at a fundamental frequency of 32 GHz. Figure 6 presents the simulated and measured output power at 64 GHz at three different DC bias conditions. The first condition (a) corresponds to class A operation, the second condition (b) is close to V_T and the third condition (c) is close to V_T and in the linear region. For these three distinct conditions, we see that the output power is accurately modelled. Unfortunately, it was not possible to apply a higher input power at 64 GHz, due to the limitations of the available hardware.

V. Conclusions

We developed an efficient procedure to generate a non-quasi-static large-signal look-up table model for InP HEMTs, that also incorporates the impact-ionisation effect. By experimental validation, we have demonstrated that the linear performance is very good up to 110 GHz and that the prediction of the output power and its harmonics is good up to at least 64 GHz.

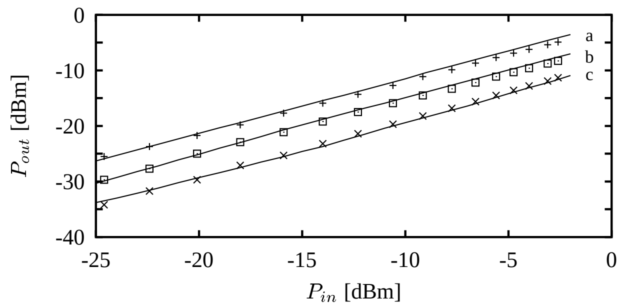

Fig. 6. Measured (symbols) and simulated (__) output power versus input power at 64 GHz and at three different bias conditions: (V_{gs}, V_{ds}) = (-0.2 V, 1 V) (a), (-0.4 V, 1 V) (b) and (-0.4 V, 0.5 V) (c).

Acknowledgement

D. Schreurs acknowledges the ETHZ Laboratory for Electromagnetic Fields and Microwave Electronics for offering her the possibility of a scientific stay as an academic guest. D. Schreurs is supported by the Fund for Scientific Research-Flanders as a Postdoctoral Fellow.

References

[1] M.H. Somerville *et al.*, "Direct correlation between impact ionization and the kink effect in InAlAs/InGaAs HEMT's", *IEEE Electron Device Letters*, pp. 473–475, 1996.

[2] D.E. Root *et al.*, "Technology independent large signal non quasi-static FET models by direct construction from automatically characterized device data", *Proc. 21th European Microwave Conf.*, pp. 927–932, 1991.

[3] C. Wei *et al.*. "Table-based dynamic FET model assembled from small-signal models", *IEEE Trans. Microwave Theory Techn.*, pp. 700–705, 1999.

[4] P. Tasker and J. Braunstein, "New MODFET small signal circuit model required for millimeterwave MMIC design: extraction and validation to 120 GHz", *Proc. IEEE MTT-S Int. Microwave Symposium*, pp. 611–614, 1995.

[5] J. Wood and D. Root, "Bias-dependent linear, scalable millimeter-wave FET model", *Proc. IEEE MTT-S Int. Microwave Symposium*, pp. 1381–1384, 2000.

[6] M. Fernandez-Barciela *et al.*, "A simplified broad-band large-signal nonquasi-static table-based FET model", *IEEE Trans. Microwave Theory Techn.*, pp. 395–405, 2000.

[7] Ph. Jansen *et al.*, "Consistent small-signal and large-signal extraction techniques for heterojunction FETs", *IEEE Trans. Microwave Theory Techn.*, pp. 87–93, 1995.

[8] R. Reuter *et al.*, "Investigation and modeling of impact ionization with regard to the RF- and noise behaviour of HFET", *Proc. IEEE MTT-S Int. Microwave Symposium*, pp. 1317–1320, 1996.

[9] D. Root, "Analysis and exact solutions of relaxation-time differential equations describing non quasi-static large signal FET models", *Proc. 24th European Microwave Conference*, pp. 854–859, 1994.

[10] D. Root, "Elements of Measurement-Based Large-signal Device Modeling", *Proc. RAWCON Workshop on Modelling and Simulation of Devices and Circuits for Wireless Communication Systems*, 34 p., 1998.

[11] D. Schreurs *et al.*, "S-Parameter measurement based quasi-static large-signal cold HEMT model for resistive mixer design", *Int. J. Microwave and Millimeter-Wave Computer-Aided Engineering*, pp. 250–258, 1996.

[12] D. Schreurs *et al.*, "DC, LF dispersion and HF characterisation of short-time stressed InP based LM-HEMTs", *Microelectronics and Reliability Journal*, pp. 1911–1914, 1996.

0-7803-6540-2/01/$10.00 (C) 2001 IEEE